Non-Luminous Flame Temperature Determination Method Based on CO_2 Radiation Intensity

S. Cięszczyk*
Institute of Electronics and Information Technology, Lublin University of Technology,
Nadbystrzycka 38A, 20-618 Lublin, Poland

(Received September 22, 2014; in final form November 4, 2014)

A new method for estimating the temperature of non-luminous flames is presented. The spectral radiation intensity emitted from uniform or temperature-axisymmetric CO_2 gas is simulated. A new inversion scheme that utilizes intensity ratios instead of directly spectral intensities is applied. This technique eliminates the errors caused by inaccuracies in the absolute radiation intensity that result from both calibration and on-site measurement. For example, this situation can occur when a spectrometer acquires radiance within only a part of its field of view. Neural networks are used as inverse models. The proposed inversion approach shows good results with simulated data. The analysis of example measured emission spectra from practical flames is also demonstrated.

DOI: 10.12693/APhysPolA.126.1235
PACS: 07.07.Df, 07.57.Ty, 33.20.Ea, 07.05.Tp

1. Introduction

The spectral remote-sensing temperature determination of hot gases is still an active research area. Temperature is an important quantity and is used to diagnose various types of industrial processes and environments. Optical methods allow for the remote quantification of homogeneous and non-homogeneous gas layers. The tomographic approach is the most appropriate in the case of a non-homogeneous path. Unfortunately, this technique requires adequate access to the test object, which is not always possible. However, an alternative line-of-sight method to determine the temperature distribution (i.e., the temperature profiles) along a one-dimensional optical path is proposed. The temperature profile can be determined from the absorption spectra, emission spectra, or both. Absorption is most commonly measured using tunable diode-laser spectroscopy (TDLS). In this method, the temperature is deduced from the ratio of two rotational gas lines, which are typically water vapor lines. The temperature distribution along the observation path can be determined by combining information from several spectral lines. Measuring the absorption, however, requires placing the transmitter and receiver on opposite sides of the gas layer. In the case of real objects, the active (laser or spectrometer) technique is not always possible to set up.

Emission (or passive) spectroscopy is called spectral remote sensing (SRS) or in some cases passive remote sensing. It is the simplest setup method because it does not require an additional radiation source; therefore, it does not require an alignment. This method is usually used to yield the atmospheric constituents and temperature. It is the simplest possible remote measurement of volcanic gases [1]. Additionally, in the case of combustion processes significant information about the processes can be obtained from their radiative emissions. The radiation from the flame consists of a continuous spectrum of soot and a discontinuous spectrum of gases primarily water vapor and CO_2. The process spectra are primarily used to analyze flame properties such as emissivity at different wavelengths and to measure the temperature [2, 3]. Pyrometry can be used to evaluate the temperature of luminous flames. A one-dimensional profile of the temperature and the soot volume fraction can be topographically reconstructed from the line-of-sight spectral emission [4]. Determining the non-luminous flame temperature is possible only in a 1–20 μm radiation range [5]. The open-path FTIR spectrometer is the most commonly used measuring instrument [6]. A special type of fiber-optic probe is utilized to monitor phenomena within the objects [7]. The fiberoptic probe counteracts the effects of atmospheric CO_2 and water vapor on the measured spectrum [8].

An interesting and currently studied remote-sensing technique for combustion processes is to analyze the spectrum of CO_2 in the 4.3 μm range [9, 10]. This method obtains the temperature profile of the nonuniform gas layer. Determining the temperature distribution on the basis of the measured spectrum is a typical inverse problem with a known physical model (i.e., a forward model) that transforms the desired quantities into directly measured quantities. Operator mapping the directly measured quantities into the desired quantities is unknown [11, 12]. Inversion algorithms are intended to minimize the differences between the measured and simulation spectra derived from the forward model. Such a formulation creates an optimization problem that arises in many similar nondestructive testing methods. Nonlinear iterative procedures for the temperature-retrieval inverse problem are used even in the case of homogeneous gas layers [13]. The key here is the calculation

*e-mail: s.cieszczyk@pollub.pl

of the CO_2 gas spectrum (a forward model). The spectrum can be modeled using line-by-line methods, such as HITEMP [14] or the simplest narrow-band models. These narrow-band models, such as statistical narrow-band (SNB) significantly reduce the computational effort and their parameters are determined from recent spectroscopic databases [15]. A simpler and faster forward model reduces the amount and time of the iterative process computation required to determine the solution [16]. Better stability of the inverse problem can be obtained using additional a priori knowledge and regularization methods [17, 18].

2. Hot-gas spectrum modelling

A homogeneous gaseous medium radiates energy if its temperature is higher than that of the surroundings. During the analysis it is assumed that light scattering from particles (e.g., soot) is not present. Light scattering significantly changes both the transmissivity and emissivity [19, 20]. Therefore the presence of particles influences the radiative emission from flames. The emissivity of a considered gas layer can be expressed as follows:

$$\varepsilon_\lambda = 1 - \exp\left(-\alpha_\lambda c l\right), \tag{1}$$

where α_λ — absorption coefficient, c — gas concentration, l — path length of the studied medium.

Considering the Planck law $L_\lambda(T)$ the intensity of the radiation can be expressed as follows:

$$I_\lambda = \varepsilon_\lambda L_\lambda(T). \tag{2}$$

Combustion radiation is dominated by a characteristic CO_2 spectrum. As considered in this article, the 4.3 μm CO_2 spectrum has special properties: its transmissivity measurement errors cause larger errors in determining the gas content than in determining the temperature [21]. Generally, temperature is more precisely retrieved than concentration for homogeneous CO2 transmission paths [22]. In some cases, the uniformity assumption is appropriate even if the test environment is evidently inhomogeneous, e.g. in flare combustion efficiency estimations [23]. A single-layer radiative transfer model is also adequate for quantifying smokestack effluent gases from coal-burning power facilities [24].

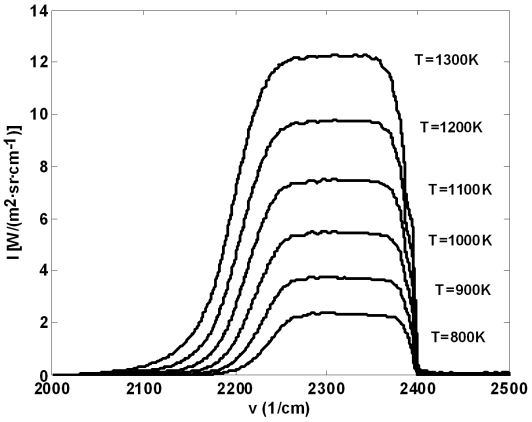

Fig. 1. Spectral intensity of uniform CO_2 gas layer.

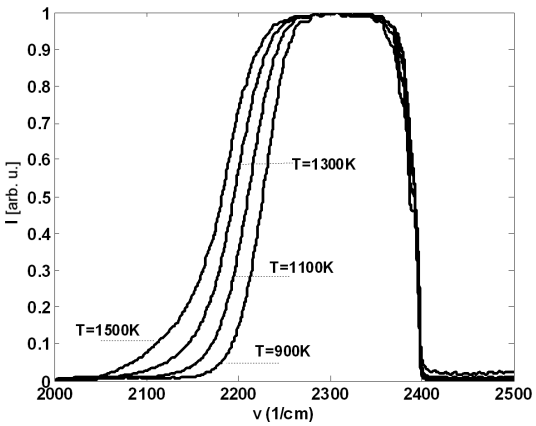

Fig. 2. Intensity spectra of the homogeneous CO_2 gas layer normalized to unity.

Modeling was performed using the HITEMP [14] database. Sample spectra of a homogeneous gas layer (with a 20 cm length and a 10% CO_2 content), in the considered range, are shown in Fig. 1. As observed, temperature changes significantly affect the intensity of the spectrum.

Temperature influences not only the intensity of the spectrum but also its shape. This effect is shown in Fig. 2 where the radiation intensity is normalized to unity.

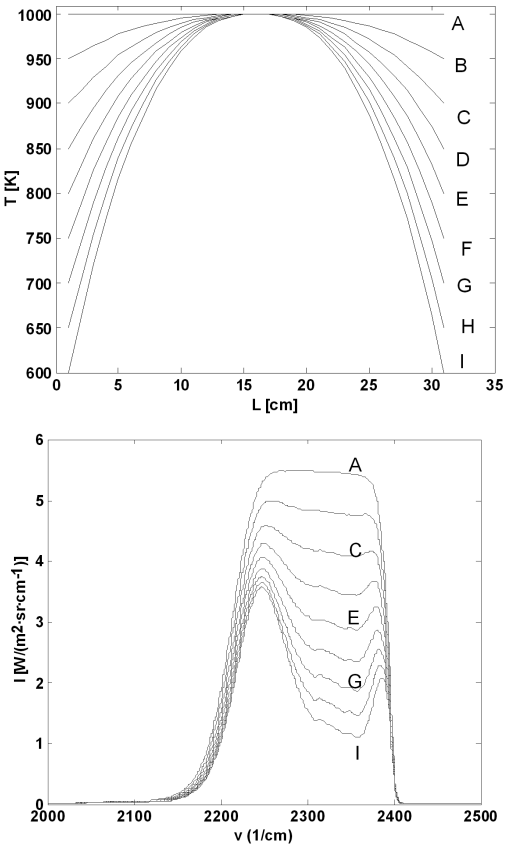

Fig. 3. Exemplary temperature distributions (top) and intensity spectra (bottom) with a 1000 K peak temperature.

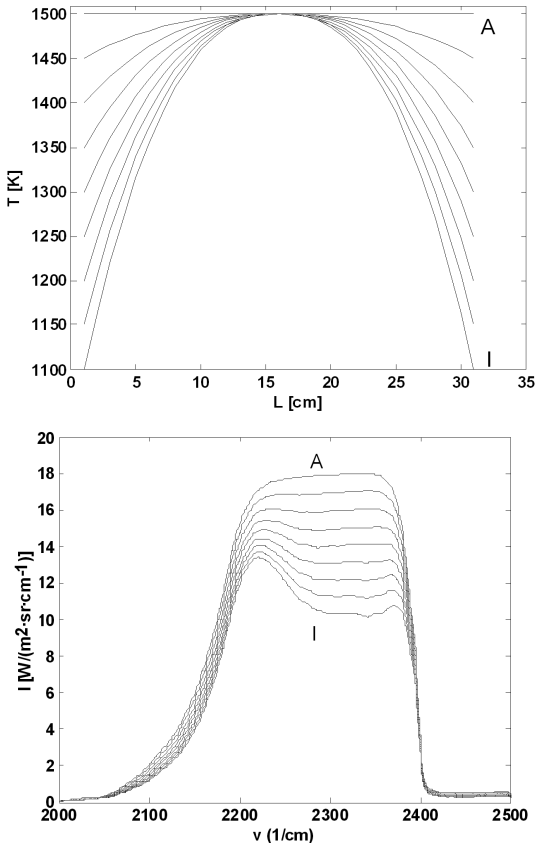

Fig. 4. Exemplary temperature distributions (top) and intensity spectra (bottom) with a 1500 K peak temperature.

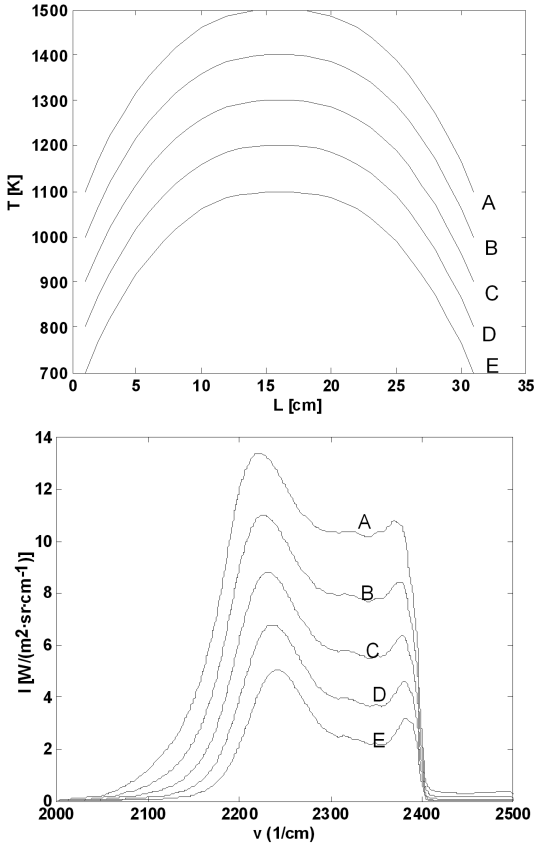

Fig. 5. Exemplary temperature distributions (top) and intensity spectra (bottom) with varying peak temperature.

The intensity spectrum calculation along the observation path by the radiative transfer equation is a forward model for a non-uniform gas slab. The radiation that reaches the spectrometer depends on the gas content and temperature distribution along the line of sight. If medium scattering and opposite wall radiation are considered not to occur, the radiation intensity can be expressed as follows:

$$I_\lambda(0) = -\int_0^L L_\lambda(T(l))\frac{\partial \tau_\lambda(l)}{\partial l}\,\mathrm{d}l, \tag{3}$$

where $\tau_\lambda(l)$ — transmissivity between spectrometer ($l = 0$) and length L of the gas path, $T(l)$ — temperature profile (distribution) along the observed path.

In-depth analysis of the studied object by a simulation forward model allows inquiring into and understanding the inverse problem without costly and difficult-to-conduct experiments [25]. The spectral radiation intensity was simulated using the radiative transfer equation and the HITEMP database. Different optical paths for various temperature distributions and CO_2 contents were studied (Figs. 3–5). The temperature distributions are axisymmetric with maximum temperatures varying from 800 K to 1500 K (Figs. 3–5). It appears that changes in the maximum temperature and the shape of the temperature distribution substantially affect the radiation intensity. The middle part of the profile, primarily the temperature peak most significantly affects the radiation intensity in the 2100–2200 cm^{-1} range. The 2250–2350 cm^{-1} range reflects the temperature near the probe (i.e., the spectrometer).

3. Determination of temperature based on the emission spectrum

Quantitative analysis of the emission spectra of varying concentrations and temperature media is not a trivial task. Similar inverse problems arise in many non-destructive diagnostic techniques e.g. bubble cloud size distribution retrieval [26], spatial distribution of intensities [27, 28], properties of composite material [29]. Their common characteristics are their complex natures and their difficulties in mathematical analysis particularly when formulating explicit relationships between measured quantities and desired quantities [30, 31]. Even interpreting the transmission spectrum of a gas slab with temperature variations is not a straightforward task [32]. In the case of the emission spectra, the simulation model which calculates the radiation intensity as a function of the temperature distribution and the gas composition is a forward problem. Our interest is in retrieving the gas content and temperature from the measured spec-

tra. The temperature profile can be determined with a specific spatial resolution. In the simplest case the optical path is divided into a predetermined number of uniform intervals. Different types of parametrization such as basis functions can also be applied [33, 34]. However, due to the similarity of the adjacent lines (or bands), the number of parameters determining the temperature distribution must be less than the number of measured bands. The issues of parametrization and spatial resolution should also be considered in terms of the measured spectral resolution, the specific applications, a priori knowledge and regularization of the method. Example high-resolution measurements for the temperature and the CO_2 concentration inversion utilize the 2379–2397 cm^{-1} (417–420 μm) spectral range [35, 36]. However, low-resolution (25 cm^{-1}) measurements give good results compared with measurements at a resolution of 0.02 cm^{-1} and suggest the possibility of shortening the measurement time and using lower-cost equipment [37].

The temperature determination is very sensitive to errors in measuring the emission intensity [38]. In part of the considered spectral range, the CO_2 radiation intensity is equal to the black-body radiation [39]. This property is used (in the 4.56–4.7 μm range) to determine the temperature in particle-laden furnaces [40]. A spectroradiometer, however, requires appropriate radiometric calibration (i.e., absolute radiometric calibration in $W\,m^{-2}\,\mu m\,sr^{-1}$ units). Errors that arise during the radiometric calibration process are primarily related to the inaccuracy of the calibration source's temperature and emissivity; these errors can be significant for even very precise instruments [41]. However, in practical measurements additional errors occur when radiation is acquired within only a part of spectrometer's field of view (FOV) or detector area. For example, the use of variable diaphragm systems changes the intensity of the radiation reaching the spectrometer [42].

Determining the temperature without absolute radiometric calibration is possible with high-resolution spectroscopy sufficient to distinguish individual spectral lines. The temperature in this case can be estimated based on the ratio of two lines. The ratio of the 4.19668 and 14.023 μm CO_2 emissions is proposed for plume temperature estimation in 310–606 K range [43]. For flame monitoring another technique must be created. The method of ratio of intensity at multiple wavelengths can be applied to eliminate the absolute spectral calibration problem. For this purpose the 11 wavelengths shown in Fig. 6 were selected. The first analyzed signal is created by the ratio of the intensities at 2230 and 2220 cm^{-1}. The second signal is the intensity ratio between 2220 and 2210 cm^{-1}. The last (10th) signal is the ratio between 2140 and 2130 cm^{-1}. Therefore, this method utilizes emission intensities similar to those encountered in multiwavelength quiet pyrometry.

The intensity ratios are temperature and CO_2content dependent. It is therefore difficult to create a mathematical model (i.e., one trying to solve the inverse problem) that specifies the temperature based on the 10 defined signals (Fig. 7). The main advantage of the inverse model construction compared with the iterative inversion method is a much faster determination of the sought quantities without multiple calculations of the forward model. The mathematical model of the considered issue as in most inverse problem cases is implicit. Therefore, the artificial neural network (ANN) universal approximation approach can be used as an inverse model. A sufficiently large data set (i.e., learning examples), representing the whole input/output relationship space, is required in neural network learning. The data can be prepared using calculations in the forward model. Network training consists of establishing the relationship between the input and output by properly setting the network weights which represent information. ANNs consist of many interconnected neurons which create layers. A single neuron output consists of the weighted inputs of every neuron in the preceding layer transformed by nonlinear activation functions.

Neural networks have been used to determine the temperature from the spectral radiation intensity [44–46]. However, these methods are based on knowing the absolute radiation intensity at various wavelengths. A mul-

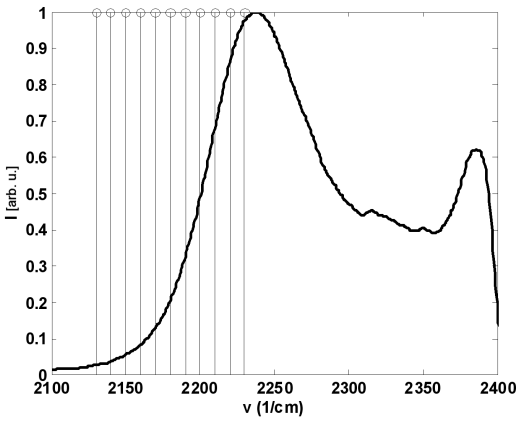

Fig. 6. Definition of the 11 considered spectral intensities.

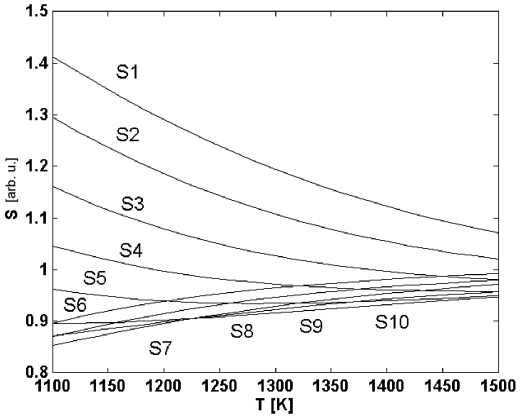

Fig. 7. Example intensity ratios for a constant concentration of CO_2.

tilayer perception neural network (with three layers) with 10 inputs (at quiet intensities) and peak temperature outputs has been selected to study. The ANN was trained by the back-propagation method, which adjusts the interconnection weights. A sigmoid was chosen as the activation function. Several temperature profiles (uniform, parabolic and other axisymmetric) were included in creating the data set. The maximum temperatures of the profiles varied from 900 to 1400 K. The CO_2 content changed from 5 to 35% across a 30 cm path length. Figure 8 shows the neural model errors for the temperature determination. The error values for specific temperatures are derived for different temperature profiles and CO_2 contents.

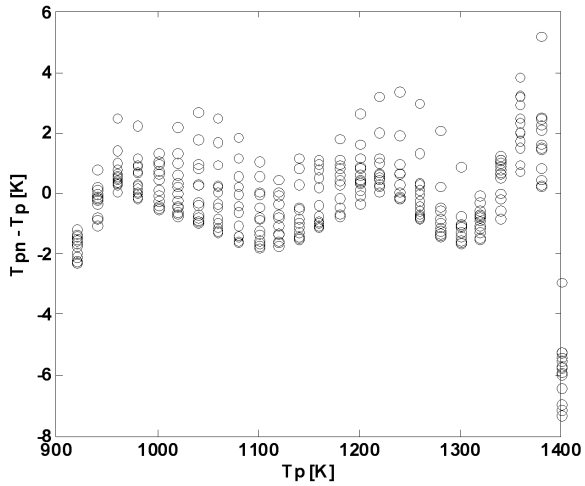

Fig. 8. Error of the neural network model for peak temperature retrieval.

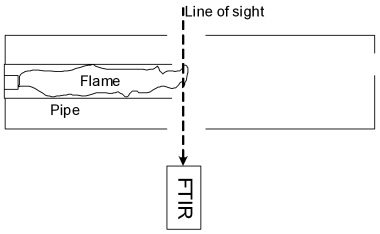

Fig. 9. Schematic diagram of the studied measurement setup.

Experiments were performed on biomass gasification and combustion sites (Fig. 9). The combustion of the gases took place in a metal tube which resulted in a uniform temperature across the flame. The radiation of the hot gases (from the tail flame) issuing from the tube was measured by a Bruker OPAG 33 spectrometer.

The measured spectrum is shown in Fig. 10. Radiation from rear wall is not present. Strong absorption in the 2300–2370 cm^{-1} range is caused by the atmospheric CO_2 between the flame and the spectrometer which was placed at a distance of 2 m.

The maximum temperature was determined using the previously built neural model. Its value is 1267 K and it overestimates the thermocouple reading by 54 K. This error results from the imprecision of the measurement and the inaccuracy in the spectrum simulation methods used. The simulation analysis of the spectrum shown in Fig. 10 as carried out in the second section indicates that the temperature distribution is almost uniform. Absorption by colder gas occurs only at the end of the measured path (Fig. 11) and by atmospheric CO_2 between the flame and the spectrometer.

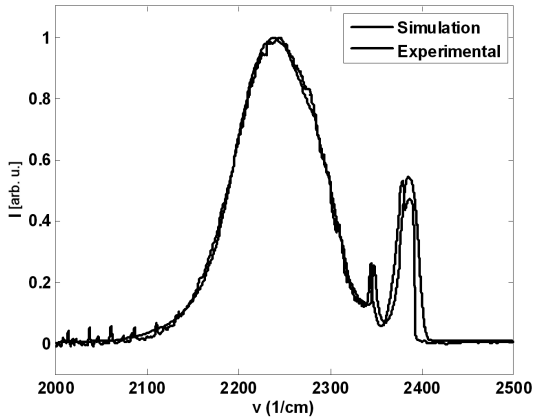

Fig. 10. Measured spectral radiation intensity of the hot gas flames.

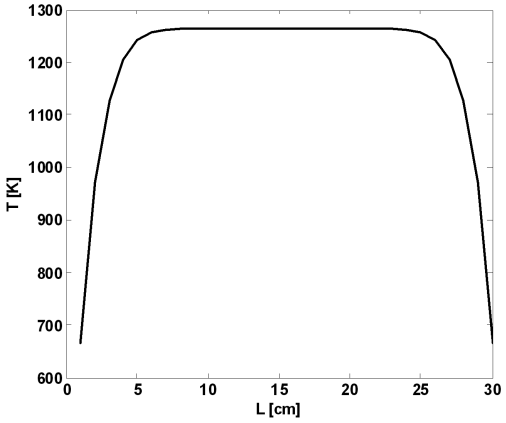

Fig. 11. Temperature distribution retrieved based on the measured emission spectra.

4. Conclusions

The remote temperature determination of non-luminous flames is based on the emission spectra of various gases. Such methods are used mainly in a laboratory investigation with high-resolution spectroscopy. Literature reports about spectral measurement and their quantitative interpretations of practical combustion processes are relatively rare. In such cases, the spectra are interpreted based on the absolute spectral radiance. This article shows the possibility of determining the temperature profile (for an assumed type of heterogeneity) and the gas content based on the shape of the emission spectrum (i.e., the ratio of the intensities of multiple wavelengths). As a forward model, a one-dimensional non-uniform gaseous environment radiation model was constructed using the radiative energy transfer equations.

A neural network inverse model was built and evaluated based on simulated data from the forward model. Practical flame spectra were measured using an FTIR spectrometer. The desired parameters were determined using a neural inversion model and comparing the measured and simulated spectra. However, a priori knowledge of the possible shape of the analyzed temperature profile in the inversion process is required. It can be assumed that in the practical application of this method to a specific issue such knowledge is available.

References

[1] S.P. Love, F. Goff, S.C. Schmidt, D. Counce, D. Pettit, B.W. Christenson, C. Siebe, *Geophysical Monograph* **116**, 117 (2000).

[2] P. Boulet, G. Parent, Z. Acem, A. Kaiss, Y. Billaud, B. Porterie, Y. Pizzo, C. Picard, *J. Combust.* **2011**, 137437 (2011).

[3] G. Parent, Z. Acem, S. Lechene, P. Boulet, *Int. J. Thermal Sci.* **49**, 555 (2010).

[4] I. Ayranci, R. Vaillon, N. Selcuk, F. Andre, D. Escudie, *J. Quant. Spectrosc. Radiat. Transfer* **104**, 266 (2007).

[5] Z. Jin, M. Yang, G. Yuan, J. Dai, *Chin. Opt. Lett.* **3**, 549 (2005).

[6] B. Wan, G.W. Small, *Analyst* **133**, 1776 (2008).

[7] J. Bak, S. Clausen, *Measur. Sci. Technol.* **13**, 150 (2002).

[8] E. Vitkin, O. Zhdanovich, V. Tamanovich, V. Senchenko, V. Dozhdikov, M. Ignatiev, I. Smurov, *Int. J. Heat Mass Transf.* **45**, 1983 (2002).

[9] H.K. Kim, T.H. Song, *J. Quant. Spectrosc. Radiat. Transf.* **73**, 517 (2002).

[10] T.H. Song, *Heat Transf. Eng.* **29**, 417 (2008).

[11] J. Mroczka, D. Szczuczyński, *J. Quant. Spectrosc. Radiat. Transf.* **129**, 48 (2013).

[12] J. Mroczka, D. Szczuczyński, *Appl. Opt.* **51**, 1715 (2012).

[13] J. Lim, Y. Sivathanu, J. Ji, J. Gore, *Combust. Flame* **137**, 222 (2004).

[14] L.S. Rothman, I.E. Gordon, R.J. Barber, H. Dothe, R.R. Gamache, A. Goldman, V.I. Perevalov, S.A. Tashun, J. Tennyson, *J. Quant. Spectrosc. Radiat. Transf.* **111**, 2139 (2010).

[15] P. Riviere, A. Soufiani, *Int. J. Heat Mass Transf.* **55**, 3349 (2012).

[16] S.W. Woo, T.H. Song, *Int. J. Thermal Sci.* **41**, 883 (2002).

[17] J. Mroczka, D. Szczuczyński, *Appl. Opt.* **49**, 4591 (2010).

[18] G. Świrniak, G. Głomb, J. Mroczka, *Appl. Opt.* **53**, 7103 (2014).

[19] M. Czerwiński, J. Mroczka, T. Girasole, G. Gouesbet, G. Grehan, *Appl. Opt.* **40**, 1514 (2001).

[20] M. Czerwiński, J. Mroczka, T. Girasole, G. Gouesbet, G. Grehan, *Appl. Opt.* **40**, 1525 (2001).

[21] T. Ren, T.A. Reeder, M.F. Modest, *Proc. ASME* **HT2013-17503**, V001T01A006 (2013).

[22] T. Ren, T.A. Reeder, M.F. Modest, *Proc. ASME* **IMECE2013-64973**, V08AT09A045 (2013).

[23] J. Wormhoudt, S.C. Herndon, J. Franklin, E.C. Wood, B. Knighton, S. Evans, C. Laush, M. Sloss, R. Spellicy, *Industr. Eng. Chem. Res.* **51**, 12621 (2012).

[24] K.C. Gross, K.C. Bradley, G.P. Perram, *Environm. Sci. Technol.* **44**, 9390 (2010).

[25] J. Mroczka, *Measurement* **46**, 2896 (2013).

[26] F. Onofri, M. Krzysiek, J. Mroczka, K. Ren, S. Radev, J. Bonnet, *Experim. Fluids* **47**, 721 (2009).

[27] J. Mroczka, D. Wysoczański, *Opt. Eng.* **39**, 763 (2000).

[28] T. Girasole, H. Bultynck, G. Gouesbet, G. Gréhan, F. Le Meur, J.N. Le Toulouzan, J. Mroczka, K.F. Ren, C. Rozé, D. Wysoczanski, *Particle Particle Syst. Character.* **14**, 163 (1997).

[29] T. Girasole, G. Gouesbet, G. Gréhan, J.N. Le Toulouzan, J. Mroczka, K.F. Ren, D. Wysoczanski, *Particle Particle Syst. Character.* **14**, 211 (1997).

[30] G. Swirniak, G. Głomb, J. Mroczka, *Appl. Opt.* **53**, 4239 (2014).

[31] T. Girasole, J. Le Toulouzan, J. Mroczka, D. Wysoczanski, *Rev. Sci. Instrum.* **68**, 2805 (1997).

[32] S. Cięszczyk, *Bull. Pol. Acad. Sci. Techn. Sci.* **62**, 33 (2014).

[33] H.K. Kim, T.H. Song, *J. Quant. Spectrosc. Radiat. Transf.* **86**, 181 (2004).

[34] H.K. Kim, T.H. Song, *J. Quant. Spectrosc. Radiat. Transf.* **93**, 369 (2005).

[35] P. Al Khoury, G. Chavent, F. Clement, P. Herve, *Inverse Probl. Sci. Eng.* **13**, 219 (2005).

[36] I. Darbord, J. Vally, E.A. Artioukhine, P. Herve, in: *Proc. 3rd Int. Conf. on Inverse Problems in Engineering, Port Ludlow (WA, USA)*, 1999.

[37] A. Soufiani, J. Martin, J. Rolon, L. Brenez, *J. Quant. Spectrosc. Radiat. Transf.* **73**, 317 (2002).

[38] J. Spelman, T.E. Parker, C.D. Carter, *J. Quant. Spectrosc. Radiat. Transf.* **76**, 309 (2003).

[39] S. Clausen, J. Bak, *Measur. Sci. Technol.* **13**, 1223 (2002).

[40] S. Rego-Barcena, R. Saari, R. Mani, S. El-Batroukh, M.J. Thomson, *Measur. Sci. Technol.* **18**, 3479 (2007).

[41] V. Tank, *J. Mol. Struct.***482-483**, 545 (1999).

[42] R. Bourayou, R. Vaillon, J.F. Sacadura, *Exp. Thermal Fluid Sci.* **26**, 181 (2002).

[43] G.P. Jellison, D.P. Miller, *Opt. Eng.* **45**, 016201 (2006).

[44] E. Garcia-Cuesta, I.M. Galvan, A.J. de Castro, in: *Proc. CIMCA-IAWTIC'05*, Ed. M. Mohammadian, IEEE Computer Society, Los Alamitos 2005, p. 81.

[45] E. Garcia-Cuesta, F. de la Torre, A.J. de Castro, in: *Proc. World Congress on Engineering and Computer Science, WCECS 2007*, Eds.: S.I. Ao, C. Douglas, W.S. Grundfest, L. Schruben, X. Wu, Newswood Limited, Hong Kong 2007, p. 683.

[46] E. Garcia-Cuesta, I.M. Galvan, A.J. de Castro, *Eng. Appl. Artific. Intell.* **21**, 26 (2008).